

Sellmann J, Lai J, Kempf AM, Chakraborty N.

[Flame Surface Density based modelling of head-on quenching of turbulent premixed flames.](#)

Proceedings of the Combustion Institute (2016)

DOI: <http://dx.doi.org/10.1016/j.proci.2016.07.114>

Copyright:

© 2016 The Author(s). Published by Elsevier Inc. on behalf of The Combustion Institute. Open Access funded by Engineering and Physical Sciences Research Council, under a Creative Commons [license](#)

Date deposited:

20/12/2016



This work is licensed under a [Creative Commons Attribution 4.0 International License](#)



Flame surface density based modelling of head-on quenching of turbulent premixed flames

Johannes Sellmann^{a,*}, Jiawei Lai^b, Andreas M Kempf^a,
Nilanjan Chakraborty^b

^a Universität Duisburg-Essen, Faculty of Engineering, Carl-Benz-Str. 199, D-47057 Duisburg, Germany

^b Newcastle University, School of Mechanical and Systems Engineering, Stephenson Building, Claremont Road, Newcastle Upon Tyne, NE1 7RU, UK

Received 2 December 2015; accepted 27 July 2016

Available online xxx

Abstract

The near-wall behaviour of the generalised flame surface density (FSD) transport in the context of Reynolds Averaged Navier–Stokes (RANS) simulations has been analysed for different values of global Lewis number using three-dimensional Direct Numerical Simulation (DNS) data of head-on quenching of statistically planar turbulent premixed flames by an isothermal inert wall. It has been found that the statistical behaviour of the FSD based reaction rate closure and the terms of the FSD transport equation are significantly affected by the presence of the wall and by the global Lewis number. The near-wall predictions of the standard FSD based mean reaction rate closure and existing sub-models for the unclosed terms of the FSD transport equation have been found to be inadequate based on *a-priori* DNS assessment, and modifications to these models have been suggested so that the predictions of modified models for reaction rate closure and FSD transport remain satisfactory, both close to the wall and away from it over a wide range of global Lewis number.

© 2016 by The Combustion Institute. Published by Elsevier Inc.

Keywords: Flame surface density (FSD); Reynolds averaged Navier–Stokes simulations (RANS); Direct numerical simulation (DNS); Head-on quenching; Lewis number

1. Introduction

Direct Numerical Simulation (DNS) contributed significantly to the fundamental under-

standing of combustion but relatively limited effort has been directed to the analysis of wall-bounded reacting flows [1–7]. Poinot et al. [3] conducted two-dimensional DNS simulations of “head-on quenching” (HOQ) of turbulent premixed flames, and reported a significant modification of the vorticity field within the flame front due to the presence of a wall. Bruneaux et al. [4,5] conducted three-dimensional incompressible DNS simulations of a “sidewall quenching” (SWQ) configuration for a premixed flame in a channel

* Corresponding author.

E-mail addresses: johannes.sellmann@uni-due.de (J. Sellmann), j.lai@newcastle.ac.uk (J. Lai), andreas.kempf@uni-due.de (A.M. Kempf), nilanjan.chakraborty@newcastle.ac.uk (N. Chakraborty).

<http://dx.doi.org/10.1016/j.proci.2016.07.114>

1540-7489 © 2016 by The Combustion Institute. Published by Elsevier Inc.

flow configuration. The data obtained from the simulations by Bruneaux et al. [4] was used to analyse a flame surface density (FSD) based reaction rate closure [5]. The near-wall behaviour of a V-flame anchored in a channel flow with isothermal walls was investigated by Alshalaan and Rutland [1,6] and Gruber et al. [7]. Alshalaan and Rutland [6] analysed the near-wall statistics of FSD as well as turbulent scalar transport and wall heat flux.

The FSD quantifies the flame surface area per unit volume of the flame [8], and is often used for the mean chemical reaction rate closure in turbulent premixed flames for both Reynolds Averaged Navier–Stokes (RANS) [9–14] and Large Eddy Simulations (LES) [15–22]. The FSD can either be modelled using an algebraic expression [9,15,17,21] or by solving a modelled transport equation [10–14,16,18,19,22]. The current analysis will focus on the RANS modelling of FSD based mean reaction rate closure in the near-wall region alongside the modelling of the unclosed terms in the transport equation for the generalised FSD (i.e. $\Sigma_{gen} = |\nabla c|$ [15], where c is the reaction progress variable and the over-bar denotes Reynolds averaging operation). The case considered is HOQ of statistically planar turbulent premixed flames by an inert isothermal wall for different values of global Lewis number Le (i.e. ratio of thermal diffusivity to mass diffusivity). It is worth noting that most LES simulations reduce to RANS in the near-wall region so that the present analysis will also be relevant to LES. The effects of turbulent Reynolds number Re_t and global Lewis number Le on the statistical behaviour of Σ_{gen} away from the wall have been investigated in a number of recent studies [11–14], which indicated that the qualitative behaviour of the FSD is unaffected by Re_t , but that the relative contributions of the unclosed terms of the FSD Σ_{gen} transport equation are affected to some extent. By contrast, Le may influence both the qualitative and quantitative behaviour of the unclosed terms [11–13]. Furthermore, the conventional FSD based closure for the mean reaction rate ($\bar{\omega} = \rho_0 S_L \Sigma_{gen}$ with the unburned gas density ρ_0 , and the unstrained laminar burning velocity S_L) is likely to underpredict (overpredict) $\bar{\omega}$ for flames with $Le < 1$ ($Le > 1$) respectively [13]. Although the near-wall behaviour of FSD based closures has been addressed in the past [5,6], the effects of turbulence intensity and Le on near-wall FSD modelling of FSD have not yet been considered. This paper addresses this gap by analysing three-dimensional DNS data of HOQ of statistically planar turbulent premixed flames by an inert isothermal wall.

2. Mathematical background

The chemical mechanism is simplified in this study by a single-step Arrhenius-type reaction in

order to permit extensive parametric analysis. Several FSD based analyses [5,6,9–22] have already been carried out using single step chemistry, and some of these closures have been demonstrated to be successful in capturing experimental observations [20–22]. Furthermore, the usage of simple chemistry allows for the analysis of Lewis number effects in isolation, which was followed in several previous analyses (see [11,13] and references therein). Detailed chemistry and transport, on the other hand, would lead to an accurate description of wall quenching for the specific set of parameters, but not for general cases. Previous analyses [3,23,24] demonstrated that experimentally obtained wall heat flux and quenching distance [25–27] can be accurately predicted using simple chemistry.

A reaction progress variable $c = (Y_{R0} - Y_R) / (Y_{R0} - Y_{R\infty})$ is defined based on a suitable reactant mass fraction Y_R where the subscripts 0 and ∞ denote the values in the fresh and burned gas, respectively. In RANS, the progress variable transport takes the following form:

$$\partial(\bar{\rho}\tilde{c})/\partial t + \partial(\bar{\rho}\tilde{u}_j\tilde{c})/\partial x_j = \bar{\omega} + \nabla \cdot (\bar{\rho}D\nabla c) - \partial(\overline{\rho u_j'' c''})/\partial x_j \quad (1)$$

Here u_j denotes the j th component of the velocity vector, ρ and D are density and diffusivity of the progress variable respectively, and $\tilde{\varphi} = \bar{\rho}\tilde{\varphi}/\bar{\rho}$ and $\varphi'' = \varphi - \tilde{\varphi}$ are the Favre-mean and -fluctuation of a general quantity φ respectively. The combined reaction rate and molecular diffusion term can be modelled as: $\bar{\omega} + \nabla \cdot (\bar{\rho}D\nabla c) = (\bar{\rho}S_d)_s \Sigma_{gen}$ where $(\bar{\varphi})_s = \bar{\varphi}|\nabla c|/|\nabla c|$ denotes surface averaging [15] and $S_d = (Dc/Dt)/|\nabla c|$ is the local displacement speed. For unity Lewis number flames the model $(\bar{\rho}S_d)_s \approx \rho_0 S_L$ is often applied [13,16,21,22]. The transport equation for Σ_{gen} takes the following form [10–14,16,18,19,22]:

$$\begin{aligned} \partial \Sigma_{gen} / \partial t + \partial (\tilde{u}_j \Sigma_{gen}) / \partial x_j &= -\partial \left\{ \underbrace{\left[(\overline{u_i})_s - \tilde{u}_i \right] \Sigma_{gen}}_{T_1 - \text{turbulent transport}} \right\} / \partial x_i \\ &+ \underbrace{\left((\delta_{ij} - N_i N_j) \partial u_i / \partial x_j \right)_s \Sigma_{gen}}_{T_2 - \text{strain rate}} \\ &- \underbrace{\partial \left[(\overline{S_d N_i})_s \Sigma_{gen} \right] / \partial x_i}_{T_3 - \text{propagation}} + \underbrace{(\overline{S_d \partial N_i / \partial x_i})_s \Sigma_{gen}}_{T_4 - \text{curvature}} \quad (2) \end{aligned}$$

Here $\vec{N} = -\nabla c / |\nabla c|$ is the local flame normal vector. The terms $T_1 - T_4$ are unclosed and thus need modelling. The near-wall modelling of $T_1 - T_4$ will be addressed in Section 4 of this paper.

Table 1

List of initial simulation parameters away from the wall.

Case	u'/S_L	l/δ_{th}	Da	Ka
A	5.0	1.67	0.33	8.67
B	6.25	1.44	0.23	13.0
C	7.5	2.50	0.33	13.0
D	9.0	4.31	0.48	13.0
E	11.25	3.75	0.33	19.5

3. Numerical implementation

The DNS have been carried out using the well-known code SENGa [17–19]. The domain size is taken as $70.6\delta_Z \times 35.2\delta_Z \times 35.2\delta_Z$, where $\delta_Z = \alpha_{T0}/S_L$ and α_{T0} are the Zel'dovich flame thickness and the thermal diffusivity in the unburned gas, respectively. The domain is discretized by a uniform Cartesian grid of $512 \times 256 \times 256$ cells, which ensures at least 10 grid points across the thermal flame thickness δ_{th} defined with the dimensional temperature \hat{T} , adiabatic flame temperature T_{ad} , and the unburned gas temperature T_0 as: $\delta_{th} = (T_{ad} - T_0)/\text{Max}|\nabla \hat{T}|_L$. The mean flame propagation is aligned with the negative x_1 -direction, i.e. towards the isothermal no-slip inert wall with temperature $T_w = T_0$. The mass flux in the wall normal direction is zero, and the boundary opposite to the wall is partially non-reflecting. Periodic boundaries are specified in the transverse directions (x_2 and x_3). High-order finite-difference and explicit Runge–Kutta schemes are used for spatial differentiation and time-advancement respectively.

Since flame-wall interaction is highly relevant to Internal Combustion (IC) engines, and all conventional hydrocarbon fuels for IC engines have Le close to unity, three different global Lewis numbers close to unity (i.e. $Le = 0.8, 1.0, 1.2$) have been considered for this analysis. Standard values were assumed for the Zel'dovich number $\beta = T_{ad}(T_{ad} - T_0)/T_0^2 = 6.0$, the Prandtl number $Pr = 0.7$ and the ratio of specific heats $\gamma = 1.4$. The heat release parameter τ is taken to be $\tau = (T_{ad} - T_0)/T_0 = 6.0$. The velocity field away from the wall has been initialised by an homogeneous isotropic incompressible turbulence field, superimposed on top of an unstrained planar laminar flame solution. For each Le , simulations have been carried out for the turbulence parameters in Table 1, which shows the initial values of normalized root mean square value of turbulent velocity u'/S_L , normalized integral length scale l/δ_{th} , Damköhler number $Da = lS_L/\delta_{th}u'$ and Karlovitz number $Ka = (u'/S_L)^{3/2} (l/\delta_{th})^{-1/2}$ away from the wall.

The values of u'/S_L and l/δ_{th} are representative of the thin reaction zone regime [28], and of ultra-lean mode Gasoline Direct Injection engine operation [29]. The simulation time varies for different values of Le and u'/S_L , as each of the simu-

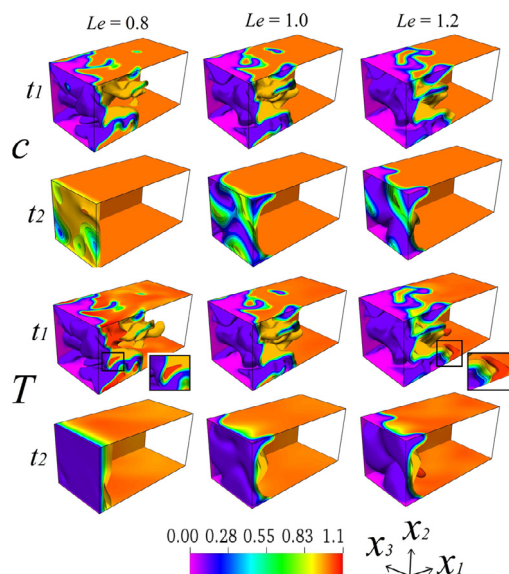


Fig. 1. Instantaneous c and T fields for case E at $t_1 = 2.18\delta_Z/S_L$ and $t_2 = 6.38\delta_Z/S_L$.

lations was run until the minimum, maximum and mean wall heat fluxes assumed identical values after quenching. It has been ensured that each simulation was continued for $t \geq 12\delta_Z/S_L$, or 15–30 initial eddy turn over times (i.e. $15 - 30l/u'$). Ensemble averaging of any quantity ϕ in a wall parallel plane at x_1 is done for the evaluation of $\bar{\phi}$ and $\hat{\phi}$.

4. Results & discussion

Figure 1 presents fields of reaction progress variable c and non-dimensional temperature $T = (\hat{T} - T_0)/(T_{ad} - T_0)$ at two different time instances ($t = 2.18\delta_Z/S_L$ and $6.38\delta_Z/S_L$) for case E.

It shows that c and T fields are considerably different from each other close to the wall for all values of Le . For globally adiabatic flames at $Le = 1.0$ and low Mach number, c is identical to T , but not in the near-wall region even for $Le = 1.0$, which is consistent with previous findings [3]. Figure 1 also shows that $T \neq c$ even when the flame is away from the wall (e.g. $t = 2.18\delta_Z/S_L$) for $Le \neq 1.0$ flames. Furthermore, the c field shows higher values at the wall for flames with smaller values of Le , which is indicative of greater extent of flame quenching for smaller Le at a given instant of time. A higher extent of flame wrinkling and faster flame propagation at lower Le brings the flame fingers closer to the wall where it eventually quenches due to heat loss through the wall [24]. It has been found that chemical reaction vanishes in a region given by $x_1/\delta_Z < Pe_{min}$ where Pe_{min} is the minimum Peclet number (where $Pe = X/\delta_Z$ is the wall Peclet number with the wall normal distance X of

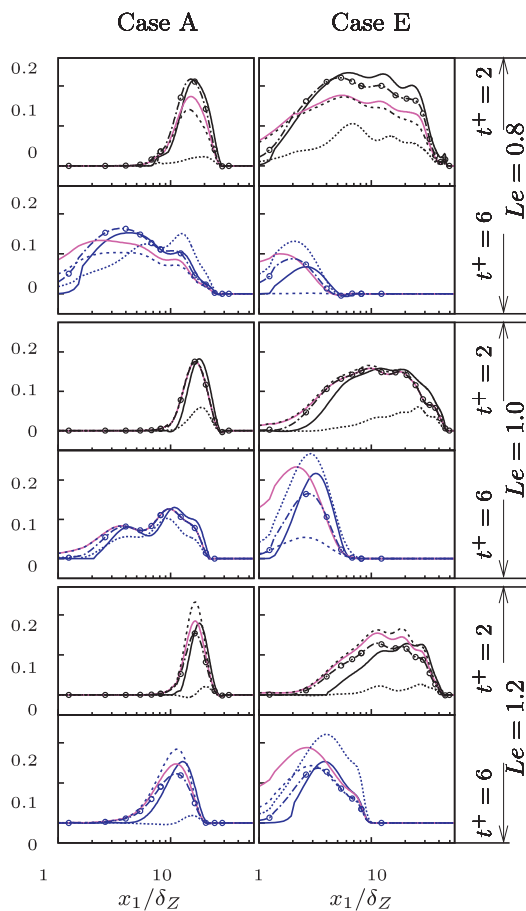


Fig. 2. Variations of the normalised mean reaction rate $\bar{\omega} \times \delta_Z / \rho_0 S_L$ (solid line), along with the predictions of $\rho_0 S_L \Sigma_{gen} \times \delta_Z / \rho_0 S_L$ (solid line), $Q_m \rho_0 S_L \Sigma_{gen} \times \delta_Z / \rho_0 S_L$ (dashed line), Alshaalan and Rutland [6] model (dotted line), and $A_1(\rho_0 S_L / Le) \Sigma_{gen} \times \delta_Z / \rho_0 S_L$ (dashed circle line) at different $t^+ = t S_L / \delta_Z = 2$ (—); 6 (—). The same colour key applies for Figs. 3, 4 and 6.

the $T = 0.9$ isosurface [3,24]). This can be substantiated from Fig. 2, which shows the distribution of $\bar{\omega} \times \delta_Z / \rho_0 S_L$ with x_1 / δ_Z at different time instants for cases A and E, which here represent the lowest and highest turbulence intensity cases respectively. Cases B and D show qualitatively similar behaviour as cases A and E respectively, and thus are not shown in Figs. 2–6. The intermediate case C is not shown here for conciseness but presented in supplemental material. The minimum Peclet number for head-on quenching of laminar premixed flames has been found to be $(Pe_{min})_L = 3.09$, 2.83 and 2.75 for $Le = 0.8$, 1.0 and 1.2, respectively [24]. These values are consistent with previous computational [3] and experimental [25–27] analyses. The minimum wall Peclet number Pe_{min} for turbulent flames

remains comparable to the corresponding laminar flame value $(Pe_{min})_L$ for $Le = 1.0$ and 1.2 cases, but for $Le = 0.8$ cases, Pe_{min} assumes a smaller magnitude than the corresponding $(Pe_{min})_L$. Lai and Chakraborty [24] parameterised Pe_{min} in turbulent flames as $\Pi = 0.5(Pe_{min})_L(\text{erf}(8Le - 6) + 1)$, which is utilised subsequently in this paper. Interested readers are referred to Lai and Chakraborty [24] for a detailed discussion of the effects of Le on wall heat flux and Pe in HOQ, which will not be repeated here for the sake of brevity.

4.1. Closure for the mean reaction rate $\bar{\omega}$

Figure 2 shows that before the onset of HOQ, $\rho_0 S_L \Sigma_{gen}$ predicts $\bar{\omega}$ satisfactorily for $Le = 1.0$ but underpredicts (overpredicts) $\bar{\omega}$ for $Le = 0.8$ ($Le = 1.2$). This is consistent with previous findings [13], which suggested that $(\rho S_d)_s$ is not approximated well by $\rho_0 S_L$ in non-unity Lewis number flames. Moreover, $\rho_0 S_L \Sigma_{gen}$ overpredicts $\bar{\omega}$ when the flame approaches the wall for all Le cases because high magnitudes of ∇c occur in the near-wall region, whereas the temperature is not sufficient to support chemical reaction. As a result, $\rho_0 S_L \Sigma_{gen} = \rho_0 S_L |\nabla c|$ overpredicts $\bar{\omega}$ in the near-wall region during flame quenching, which is consistent with previous findings [5,6]. Alshaalan and Rutland [6] proposed the near-wall modification: $\Sigma_{gen} = |\nabla c|(1 + c_y \tilde{A}_w) \times \exp[-\beta(\tau \tilde{A} / ((1 + \tau \tilde{T})(1 + \tau \tilde{c})))^{c_x}]$ where $c_x = 0.25$ and $c_y = 48$ are the model parameters, $\tilde{A} = (\tilde{c} - \tilde{T})$ is a non-adiabaticity parameter and $\tilde{\phi}_w$ is the Favre-average of a general quantity ϕ at the wall. This modification leads to a significant underprediction of $\bar{\omega}$ when the flame is away from the wall (see Fig. 2), whereas $\bar{\omega}$ is overpredicted close to the wall.

Bruneaux et al. [5] proposed a modification to the conventional $\bar{\omega}$ closure by a multiplier $Q_m = \exp[-2\beta(\tilde{c} - \tilde{T})]$ in the model expression ($\bar{\omega} = Q_m \rho_0 S_L \Sigma_{gen}$) where Q_m is unity when the flame is away from the wall but decreases in the near-wall region. However, the prediction of $Q_m \rho_0 S_L \Sigma_{gen}$ differs significantly from $\bar{\omega}$ when the flame begins to interact with the wall especially for non-unity Lewis number flames. Chakraborty and Cant demonstrated [13] that away from the wall, $(\rho S_d)_s$ can be approximated by $\rho_0 S_L / Le$. Using this, a revised closure has been proposed as $\bar{\omega} = A_1(\rho_0 S_L / Le) \Sigma_{gen}$, where $A_1 = 0.5[\text{erf}(x_1 / \delta_Z - 0.7 \Pi) + 1]$ is a wall correction that damps the magnitude of $(\rho_0 S_L / Le) \Sigma_{gen}$ in the near-wall region $x_1 / \delta_Z \ll Pe_{min}$ but asymptotically approaches unity for $x_1 / \delta_Z \gg Pe_{min}$. Figure 2 shows that $A_1(\rho_0 S_L / Le) \Sigma_{gen}$ predicts $\bar{\omega}$ satisfactorily both away from the wall and close to it. The expression $A_1(\rho_0 S_L / Le) \Sigma_{gen}$ can therefore be used to predict $\bar{\omega}$ if Σ_{gen} is modelled accurately, the closure of the transport equation terms for Σ_{gen} will be discussed next.

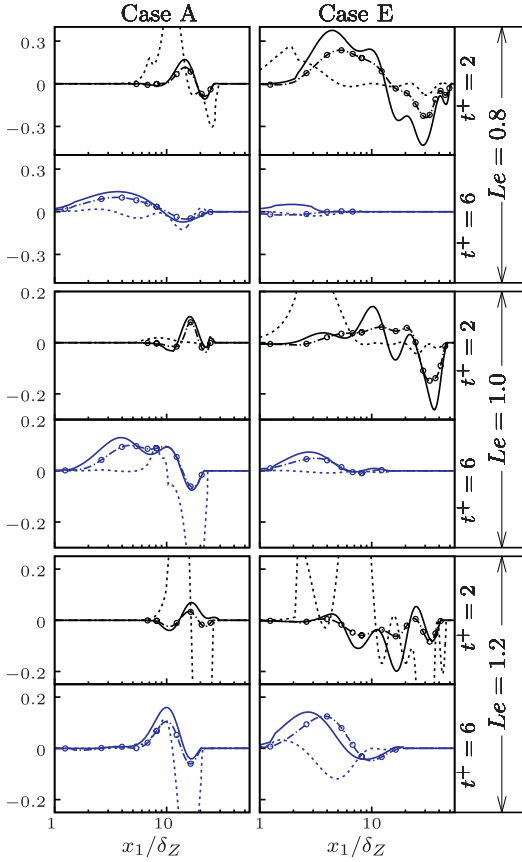


Fig. 3. Variations of the normalised turbulent flux $[(u_i)_s - \tilde{u}_i]\Sigma_{gen} \times \delta_Z/S_L$ (solid line) and the prediction of Eq. (3) (dashed line), and Eq. (4) with near-wall modification (dashed circle line) at different $t^+ = tS_L/\delta_Z$.

4.2. Modelling of the turbulent transport term T_1

The behaviour of T_1 depends on the turbulent flux $[(u_i)_s - \tilde{u}_i]\Sigma_{gen}$ and needs to be modelled. The variation of $[(u_i)_s - \tilde{u}_i]\Sigma_{gen}$ with x_1/δ_Z is shown in Fig. 3 for cases A and E at different times for $Le = \{0.8, 1.0, 1.2\}$. An increased u'/S_L leads to an increase in magnitude of $[(u_i)_s - \tilde{u}_i]\Sigma_{gen}$, whereas the magnitude of the FSD flux increases with decreasing Le . Figure 3 indicates that $[(u_i)_s - \tilde{u}_i]\Sigma_{gen}$ is significantly affected by the wall and that $[(u_i)_s - \tilde{u}_i]\Sigma_{gen}$ only exhibits positive values close to the wall before vanishing altogether following flame quenching. Bruneaux et al. [5] proposed the following gradient hypothesis model:

$$[(u_i)_s - \tilde{u}_i]\Sigma_{gen} = -(\nu_t/\sigma_\Sigma)(\partial\Sigma_{gen}/\partial x_i) \quad (3)$$

Here $\nu_t = \min(0.09\tilde{k}^2/\tilde{\epsilon}, 0.20(x(1 - e^{-x^+}/26)))\tilde{k}^{1/2}$ and σ_Σ are the eddy viscosity and turbulent Schmidt number respectively, with

$\tau_w, x^+ = \rho x(\tau_w/\bar{\rho})^{1/2}/\mu, \tilde{k} = \overline{\rho u_i'' u_i''}/2\bar{\rho}$ and $\tilde{\epsilon} = \mu(\partial u_i''/\partial x_j)(\partial u_i''/\partial x_j)/\bar{\rho}$ being the wall shear stress, the non-dimensional wall distance, turbulent kinetic energy and its dissipation rate respectively.

For $\sigma_\Sigma = 1.0$, Eq. (3) does not predict the qualitative behaviour of $[(u_i)_s - \tilde{u}_i]\Sigma_{gen}$ both far from the wall and close to it for the cases considered here, and predicts an opposite sign to that of $[(u_i)_s - \tilde{u}_i]\Sigma_{gen}$ obtained from DNS data (see Fig. (3)). This discrepancy originates from the predominantly counter-gradient behaviour of $[(u_i)_s - \tilde{u}_i]\Sigma_{gen}$ in the cases considered here. Chakraborty and Cant [13] proposed a model that also accounts for both gradient and counter gradient transport:

$$[(u_i)_s - \tilde{u}_i]\Sigma_{gen} = (A_2 - A_3\tilde{c})\overline{\rho u_i'' c''}\Sigma_{gen}/\{\overline{\rho c''^2} + \bar{\rho}\tilde{c}(1 - \tilde{c})\} \quad (4)$$

Equation 4 with the model parameters $A_2 = 1.0$ and $A_3 = 2.0$ shows a satisfactory behaviour away from the wall but it underpredicts the magnitude of $[(u_i)_s - \tilde{u}_i]\Sigma_{gen}$ close to the wall (see supplemental material). To improve the predictions of Eq. (4), the following expressions are suggested: $A_2 = 1.06 - 0.06\text{erf}(x_1/\delta_Z - 2.0\Pi)$ and $A_3 = 0.93 + 1.07\text{erf}(x_1/\delta_Z - 2.0\Pi)$ so that A_2 and A_3 approach 1.0 and 2.0, respectively, away from the wall ($x_1/\delta_Z > 2.0\Pi$), whereas they increase and decrease respectively close to the wall ($x_1/\delta_Z < 2\Pi$). Figure 3 shows that Eq. (4) with near-wall modification satisfactorily predicts the behaviour of $[(u_i)_s - \tilde{u}_i]\Sigma_{gen}$ both far from the wall and close to it.

4.3. Modelling of the tangential strain rate term T_2

The variation of T_2 with x_1/δ_Z is shown in Fig. 4 for the cases A and E at different times for $Le = \{0.8, 1.0, 1.2\}$. The term T_2 assumes positive values but its magnitude decreases with time when the flame starts to interact with the wall and eventually vanishes. Bruneaux et al. [5] used the model $T_2 = \alpha_m(\tilde{\epsilon}/\tilde{k})\Gamma(u'/S_L, l/\delta_Z)\Sigma_{gen}$ where $\alpha_m \approx 2.0$ is a model parameter and $\Gamma(u'/S_L, l/\delta_Z)$ is an efficiency function [30]. The predictions of the Bruneaux et al. [5] ($T_2 = \alpha_m(\tilde{\epsilon}/\tilde{k})\Gamma(u'/S_L, l/\delta_Z)\Sigma_{gen}$) are shown in Fig. 4: this model does not capture the qualitative behaviour of T_2 for the cases considered here and overpredicts the magnitude of T_2 . This warrants for a new modelling methodology for T_2 . The term T_2 can be decomposed [12–14] into T_D , the contribution due to dilatation $\partial u_i/\partial x_i$, and T_N , the contribution of the normal strain rate $N_i N_j \partial u_i/\partial x_j$:

$$T_2 = \underbrace{(\partial u_i/\partial x_i)_s \Sigma_{gen}}_{T_D} - \underbrace{(N_i N_j \partial u_i/\partial x_j)_s \Sigma_{gen}}_{T_N} \quad (5)$$

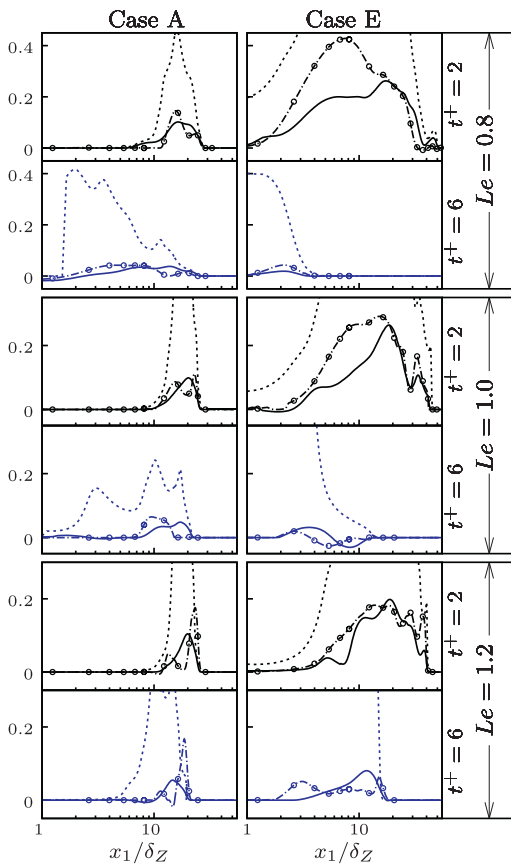


Fig. 4. Variations of the strain rate term $T_2 \times \delta_Z^2 / S_L$ (solid line) along with the predictions of the Bruneaux et al. [5] model (dashed line) and the combined outcome of the models of T_{D1} , T_{N1} , T_{D2} and T_{N2} with wall modifications (dashed circle line) at different $t^+ = tS_L/\delta_Z$.

The dilatation rate term T_D can be decomposed into the resolved T_{D1} and unresolved T_{D2} parts: $T_D = T_{D1} + T_{D2}$. The resolved part is defined [12] as: $T_{D1} = (\partial \tilde{u}_i / \partial x_i) |\nabla \tilde{c}|$, which needs evaluation of \tilde{c} from \tilde{c} . Here $\tilde{c} = (1 + \tau g^a Le^{-b}) \tilde{c} / (1 + \tau g^a Le^{-b} \tilde{c})$ is considered following previous analyses [12,13], where $a=1.5$ and $b=0.26$ are the parameters, $g = \tilde{c}^2 / [\tilde{c}(1 - \tilde{c})]$ is the segregation factor, and Le^{-b} accounts for the strengthening of heat release effects with decreasing Le . Figure 5 shows that the approximation $\tilde{c} = (1 + \tau g^a Le^{-b}) \tilde{c} / (1 + \tau g^a Le^{-b} \tilde{c})$ enables a satisfactory prediction of T_{D1} both away from the wall and close to it.

For the unresolved dilatation term $T_{D2} = (\partial u_i / \partial x_i) |\nabla c| - (\partial \tilde{u}_i / \partial x_i) |\nabla \tilde{c}|$ Katragadda et al. [12] suggested the following model:

$$T_{D2} = (\tau S_L / \delta_{th} Le^{1.845}) [A_4 \cdot (1 - \tilde{c})^\zeta (\Sigma_{gen} - |\nabla \tilde{c}|)] \quad (6)$$

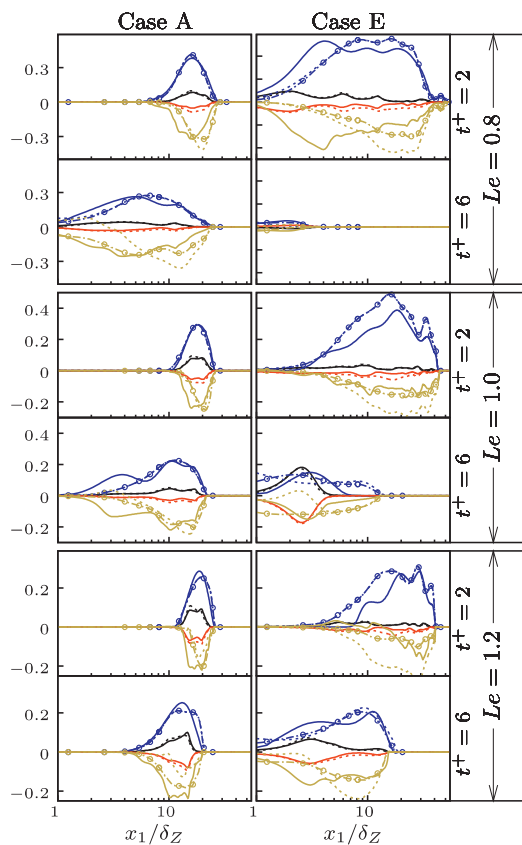


Fig. 5. Variations of $(T_{D1} (—), T_{D2} (—), -T_{N1} (—), -T_{N2} (—)) \times \delta_Z^2 / S_L$ obtained from DNS (solid line) and the model predictions according to $\tilde{c} = (1 + \tau g^a Le^{-b}) \tilde{c} / (1 + \tau g^a Le^{-b} \tilde{c})$, $(N_i N_j)_s = (N_i)_s (N_j)_s + (\delta_{ij} / 3) [1 - (N_k)_s (N_k)_s]$, Eqs. (6) and (8) respectively, with (dashed circle line) and without (dashed line) wall modifications at different $t^+ = tS_L/\delta_Z$.

The parameters are $A_4 = 1.8 / (1 + Ka_L)^{0.35}$ and $\zeta = 1.5 - 1.8 Le$, with $Ka_L = (\tilde{\epsilon} \delta_{th}) / (S_L^{1.5})$ being the local Karlovitz number. The Karlovitz number dependence of A_4 ensures weakening of dilatation effects for high values of Ka_L [12,13]. Figure 5 shows that Eq. (6) provides a satisfactory prediction of T_{D2} but the near-wall behaviour has been found to be inadequate. Here A_4 and ζ have been modified to account for the near-wall behaviour as: $A_4 = 0.9 \exp[1.2(\tilde{c}_w - \tilde{T}_w)] [\text{erf}(Le x_1 / \delta_Z) + 1] / (1 + Ka_L)^{0.35}$ and $\zeta = 1.5 \exp[0.2(\tilde{c}_w - \tilde{T}_w)] - 1.8 Le$. Note that $(\tilde{c}_w - \tilde{T}_w)$ not only accounts for non-adiabaticity induced by the wall but also acts as a quenching sensor (i.e. $(\tilde{c}_w - \tilde{T}_w)$ remains zero when the flame is away from the wall but it rises once the flame quenching is initiated). Thus, the involvement of $(\tilde{c}_w - \tilde{T}_w)$ in A_4 and ζ modifies the prediction of Eq. (6) in the near-wall region only when the flame starts to quench. The

modified parameters A_4 and ζ approach the earlier expressions [12] away from the wall. Equation (6) with the modified A_4 and ζ provides a satisfactory prediction of T_{D2} both away from the wall and near to it (see Fig. 5).

The normal strain rate term T_N can also be split into resolved (T_{N1}) and unresolved (T_{N2}) parts:

$$-T_N = -\underbrace{(\overline{N_i N_j})_s (\partial \tilde{u}_i / \partial x_j) \Sigma_{gen}}_{T_{N1}} - \underbrace{(\overline{N_i N_j \partial u_i'' / \partial x_j})_s \Sigma_{gen}}_{T_{N2}} \quad (7)$$

The resolved component T_{N1} can be closed if $(\overline{N_i N_j})_s$ is suitably modelled. Figure 5 shows that $(-T_{N1})$ can be predicted satisfactorily both away from the wall and close to it without any modification with the model: $(\overline{N_i N_j})_s = (\overline{N_i})_s (\overline{N_j})_s + (\delta_{ij}/3)[1 - (\overline{N_k})_s (\overline{N_k})_s]$ [10]. Katragadda et al. [12] suggested the following model for $(-T_{N2})$:

$$-T_{N2} = (\tilde{\epsilon}/\tilde{k})[C_1 - \tau C_2 f(Le) Da_L] \Sigma_{gen} \quad (8)$$

Here C_1 and C_2 are model parameters, $Da_L = \tilde{k} S_L / (\tilde{\epsilon} \delta_{th})$ is the local Damköhler number, and $f(Le) = \exp(Le^{-0.945} - 1)$ is a function, accounting for increased flame normal acceleration with decreasing Le [12]. The term $C_1(\tilde{\epsilon}/\tilde{k})\Sigma_{gen}$ is responsible for FSD generation due to alignment of ∇c with the most compressive principal strain rate under the action of turbulent straining ($\sim \tilde{\epsilon}/\tilde{k}$) [12]. By contrast, $-(\tilde{\epsilon}/\tilde{k})\tau C_2 Da_L \Sigma_{gen}$ accounts for FSD destruction due to the alignment of ∇c with the most extensive principal strain rate induced by flame normal acceleration ($\sim \tau f(Le) S_L / \delta_{th}$) [12]. Based on the present analysis, $C_1 = \text{erf}(0.1 x_1 / \delta_Z)$ and $C_2 = A_5(1 - (\overline{N_k})_s (\overline{N_k})_s) / (1 + Ka_L)^{0.35}$ have been proposed guided by the analysis of Katragadda et al. [12] where A_5 is given by:

$$A_5 = 0.471 \text{erf}(0.5 \cdot x_1 / \delta_Z) \exp(2.0(\tilde{c}_w - \tilde{T}_w)) \times \left[\frac{0.3}{\text{erf}(Re_L + 0.01)^{0.5 \exp(-\tilde{c}_w)}} \right]^{A_6} \quad (9)$$

In this expression $A_6 = 0.5(\text{erf}(-x_1 / \delta_Z + \Pi^3) + 1)$ and $Re_L = (\rho_0 \tilde{k}^2 / \mu_0 \tilde{\epsilon})$ is the local turbulent Reynolds number, where μ_0 is the unburned gas viscosity. The error function $\text{erf}(0.5 \cdot x_1 / \delta_Z)$ in Eq. (9) allows for the gradual increase of $(-T_{N2})$ from the wall. The combined effects from error function and exponential function in $\text{erf}(0.5 \cdot x_1 / \delta_Z) \exp(2.0(\tilde{c}_w - \tilde{T}_w))$ are needed to capture the correct magnitude in the near-wall region ($x_1 / \delta_Z < \Pi$) at all times. The expression $[0.3 / \text{erf}(Re_L + 0.01)^{0.5 \exp(-\tilde{c}_w)}]^{A_6}$ is responsible for the correct prediction of $(-T_{N2})$ away from the wall. The involvement of $(\tilde{c}_w - \tilde{T}_w)$ and \tilde{c}_w ensures that the near-wall modification takes effect

only when the flame quenching takes effect. The Karlovitz number dependence of C_2 ensures the weakening of flame normal acceleration effects for high values of Ka_L [12].

Figure 4 shows the predictions of T_2 when T_{D1} , T_{N1} , T_{D2} and T_{N2} are modelled with $\tilde{c} = (1 + \tau g^a Le^{-b}) \tilde{c} / (1 + \tau g^a Le^{-b} \tilde{c})$, $(\overline{N_i N_j})_s = (\overline{N_i})_s (\overline{N_j})_s + (\delta_{ij}/3)[1 - (\overline{N_k})_s (\overline{N_k})_s]$, Eqs. (6) and (8) respectively. This model captures qualitative and quantitative behaviour of T_2 both away from the wall and near to it, except in case E for $Le=0.8$ where a slight overprediction is observed. However, this model is more successful in capturing both qualitative and quantitative behaviours of T_2 than the Bruneaux et al. [5] model both away from and close to the wall.

4.4. Modelling of propagation and curvature terms ($T_3 + T_4$)

Several previous analyses [11–13] modelled the propagation and curvature terms together. The variation of $(T_3 + T_4)$ with x_1 / δ_Z is presented in Fig. 6 for cases A and E at different times for $Le = \{0.8, 1.0, 1.2\}$. The combined term $(T_3 + T_4)$ shows positive (negative) values towards the unburned (burned) gas side of the flame brush. Bruneaux et al. [5] proposed separate models for T_3 and T_4 ($T_3 = -\partial \{S_L M_i \Sigma_{gen} (1 - (1 - Q_m) / \gamma_\omega)\} / \partial x_i$ and $T_4 = -S_L \Sigma_{gen}^2 / \tilde{c}(1 - \tilde{c})$ with $\gamma_\omega = 0.3$, $Q_m = \exp[-2\beta(\tilde{c} - \tilde{T})]$ and the resolved flame normal vector $\vec{M} = -\nabla \tilde{c} / |\nabla \tilde{c}|$). Figure 6 shows that the Bruneaux et al. [5] model does not capture the qualitative behaviour of $(T_3 + T_4)$ obtained from DNS data.

Chakraborty and Cant [13] proposed the following model for $(T_3 + T_4)$ with the model parameters $\beta_0 = 8.0$ and $c_{cp} = 0.35$:

$$(T_3 + T_4) = -\frac{\partial}{\partial x_i} \left[\frac{\rho_0 S_L}{\tilde{\rho}} (\overline{N_i})_s \Sigma_{gen} \right] + \frac{\rho_0 S_L}{\tilde{\rho}} \frac{\partial (\overline{N_i})_s}{\partial x_i} \Sigma_{gen} - \beta_0 \left[1 - (\overline{N_k})_s (\overline{N_k})_s \right] \frac{(\tilde{c} - c_{cp}) S_L \Sigma_{gen}^2}{\tilde{c}(1 - \tilde{c})} \quad (10)$$

Equation 10 provides a satisfactory prediction away from the wall but overpredicts the magnitude of $(T_3 + T_4)$ close to the wall (see supplemental material). This deficiency is avoided when S_L in Eq. (10) is replaced by a modified flame speed $S'_L = S_L \exp[-8.0(\tilde{c} - \tilde{T})]$ and Fig. 6 shows that Eq. (10) with S'_L satisfactorily predicts $(T_3 + T_4)$ both away from the wall and close to it. The involvement of $(\tilde{c} - \tilde{T})$ in the modified flame speed S'_L accounts for the reduction in flame propagation rate during flame quenching.

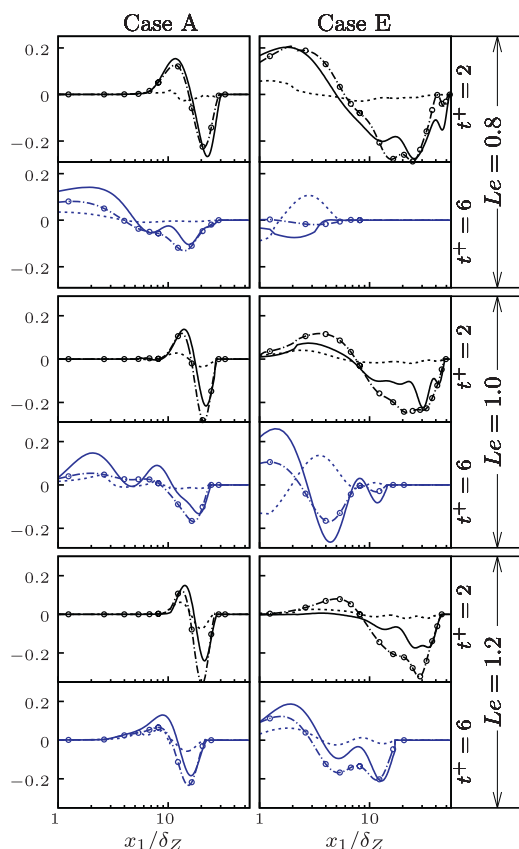


Fig. 6. Variations of the normalised curvature and propagation term $(T_3 + T_4) \times \delta_Z^2 / S_L$ obtained from DNS data (solid line) and the predictions of the Bruneaux et al. [5] model (dashed line) and Eq. (10) with near-wall modification (dashed circle line) at different $\tau^+ = t S_L / \delta_Z$.

5. Conclusions

The FSD based reaction rate closure for HOQ of statistically planar turbulent premixed flames has been analysed for three-dimensional DNS data for different values of Le . The existing models, which were proposed for the mean reaction rate and the unclosed terms of the FSD transport equation away from walls, have been found to yield inaccurate predictions in the near-wall region during flame quenching. These models have been modified for the accurate prediction in the near-wall region, based on *a-priori* analysis using explicitly Reynolds averaged DNS data. Here, following previous analyses [5,6], the near-wall modifications have been proposed in terms of the minimum Peclet number (i.e. normalised quenching distance) and the quantities $(\tilde{c} - \tilde{T})$ and $(\tilde{c}_w - \tilde{T}_w)$, which account for non-adiabaticity and flame quenching, respectively. It has been demonstrated earlier [3,23] that a different wall temperature (which amounts to a

modification of τ) does not significantly affect the minimum wall Peclet number (which has been confirmed by limited number of simulations but not shown here), and thus a modification of wall temperature is not expected to have a major influence of the performance of near-wall modifications proposed here. In this *a-priori* analysis, the newly proposed models perform better than the existing models [5], but they need to be validated further for higher turbulent Reynolds number Re_t and more detailed chemistry. Further validation of the models in actual RANS simulations for the purpose of *a-posteriori* assessment is necessary.

Acknowledgements

The authors are grateful to EPSRC (Grant number EP/K025163/1) and N8/ARCHER for the financial and computational support.

Supplementary materials

Supplementary material associated with this article can be found, in the online version, at doi:10.1016/j.proci.2016.07.114.

References

- [1] T. Alshaalan, C.J. Rutland, *Combust. Sci. Technol.* 174 (2002) 135–165.
- [2] B. Boust, J. Sotton, S.A. Labuda, M. Bellenoue, *Combust. Flame* 149 (2007) 286–294.
- [3] T.J. Poinso, D.C. Haworth, G. Bruneaux, *Combust. Flame* 95 (1993) 118–132.
- [4] G. Bruneaux, K. Akselvoll, T. Poinso, J.H. Ferziger, *Combust. Flame* 107 (1996) 27–36.
- [5] G. Bruneaux, T. Poinso, J.H. Ferziger, *J. Fluid Mech.* 349 (1997) 191–219.
- [6] T. Alshaalan, C.J. Rutland, *Proc. Combust. Inst.* 27 (1998) 793–799.
- [7] A. Gruber, R. Sankaran, E.R. Hawkes, J.H. Chen, *J. Fluid. Mech.* 658 (2010) 5–32.
- [8] S.M. Candel, T.J. Poinso, *Combust. Sci. Technol.* 70 (1990) 1–15.
- [9] R.S. Cant, K.N.C. Bray, *Proc. Combust. Inst.* 22 (1988) 791–799.
- [10] R.S. Cant, S.B. Pope, K.N.C. Bray, *Proc. Combust. Inst.* 27 (1990) 809–815.
- [11] I. Han, K.Y. Huh, *Combust. Flame* 152 (2008) 194–205.
- [12] M. Katragadda, S.P. Malkeson, N. Chakraborty, *Proc. Combust. Inst.* 33 (2011) 1429–1437.
- [13] N. Chakraborty, R.S. Cant, *Combust. Flame* 158 (2011) 1768–1787.
- [14] N. Chakraborty, R.S. Cant, *Proc. Combust. Inst.* 34 (2013) 1347–1356.
- [15] M. Boger, D. Veynante, H. Boughanem, A. Trouvé, *Proc. Combust. Inst.* 27 (1998) 917–925.
- [16] E.R. Hawkes, R.S. Cant, *Combust. Flame* 126 (2001) 1617–1629.
- [17] N. Chakraborty, R.S. Cant, *Phys. Fluids* 19 (2007) 105101.

- [18] N. Chakraborty, M. Klein, *Phys. Fluids* 20 (2008) 085108.
- [19] N. Chakraborty, R.S. Cant, *Proc. Combust. Inst.* 32 (2009) 1445–1453.
- [20] F.E. Hernández-Pérez, F.T.C. Yuen, C.P.T. Groth, Ö.L. Gülder, *Proc. Combust. Inst.* 33 (2011) 1365–1371.
- [21] T. Ma, O. Stein, N. Chakraborty, A. Kempf, *Combust. Theor. Modell.* 17 (2013) 431–482.
- [22] T. Ma, O. Stein, N. Chakraborty, A.M. Kempf, *Combust. Theor. Modell.* 18 (2014) 32–64.
- [24] T. Poinso, D. Veynante, *Theoretical and Numerical Combustion*, R.T. Edwards Inc., Philadelphia, USA, 2001.
- [24] J. Lai, N. Chakraborty, *Flow, Turb. Combust.* (2015), doi:10.1007/s10494-015-9629-x.
- [25] S.R. Vosen, R. Greif, C. Westbrook, *Proc. Combust. Inst.* 20 (1984) 76–83.
- [26] J. Jarosinsky, *Combust. Sci. Technol.* 12 (1986) 81–116.
- [27] W.M. Huang, S.R. Vosen, R. Greif, *Proc. Combust. Inst.* 21 (1986) 1853.
- [28] N. Peters, *Turbulent Combustion*, 1st edition, Cambridge University Press, Cambridge, UK, 2000.
- [29] D.C. Haworth, R.J. Blint, B. Cuenot, T.J. Poinso, *Combust. Flame* 121 (2000) 395–417.
- [30] C. Meneveau, T. Poinso, *Combust. Flame* 86 (1991) 311–332.